

Scattering of Electromagnetic Waves by Impedance Biconical Vibrators in a Free Space and in a Rectangular Waveguide

Mikhail V. Nesterenko*, Andrey V. Gomofov, Victor A. Katrich,
Sergey L. Berdnik, and Victor I. Kijko

Abstract—A problem of scattering of electromagnetic waves by thin impedance biconical vibrators in a free space and in a rectangular waveguide is solved by an asymptotic averaging method and a generalized method of induced electromotive forces (EMF). An influence of the change of vibrator radius upon energy and spatial characteristics is numerically studied. Theoretical results are compared with the experimental data.

1. INTRODUCTION

An additional parameter for obtaining the given electrodynamic characteristics of cylindrical vibrator antennas can be a change in the radius of the cross section of the vibrator along its length. Such radiators (scatterers) can be located in free space, half-space, a rectangular waveguide or a resonator. If the radius of the vibrator increases from the center of the antenna to its ends according to a linear law (biconic vibrator), then such an antenna resonates at a smaller geometric length and is more broadband than a vibrator of constant radius. Starting from the classic publication of Shchelkunov [1], antennas of this type have attracted the attention of many researchers (see, for example, [2–10] and references to them); however, all of them are devoted to calculating the characteristics of a radiating vibrator excited at the center by a concentrated EMF. At the same time, to analyze the receiving antennas, it is necessary to know the induced current in a scattering vibrator excited by an incident electromagnetic wave. This problem is also of independent applied importance in the study of the scattering characteristics of material bodies of complex configuration [11].

In this article, solutions for problems of electromagnetic wave scattering by thin impedance vibrators of variable cross-sectional radius located in free space and in a rectangular waveguide are obtained. Moreover, for clarity and comparative analysis, the solutions were carried out by different methods. The electrodynamic characteristics of such antennas are investigated and compared with experimental data.

2. IMPEDANCE BICONICAL VIBRATORS IN A FREE SPACE

2.1. Problem Formulation and Initial Integral Equations

Let us limit ourselves by the linear law of the radius change along the vibrator (Fig. 1), which, in its turn, is rather good approximation and for another dependence $r(s)$, for example, exponential one, at small angles ψ . Let the impedance vibrator of $2L$ length and $r(s)$ variable radius, located in free space, be excited by the plane electromagnetic wave with E_0 amplitude. The monochromatic fields and

Received 3 February 2022, Accepted 31 March 2022, Scheduled 23 April 2022

* Corresponding author: Mikhail V. Nesterenko (mikhail.v.nesterenko@gmail.com).

The authors are with the Department of Radiophysics, Biomedical Electronics and Computer Systems, V. N. Karazin Kharkiv National University, 4, Svobody Sq., Kharkiv 61022, Ukraine.

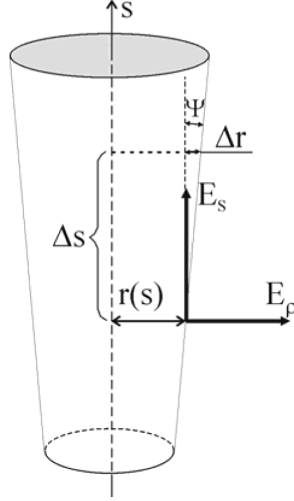


Figure 1. The vibrator fragment of the variable radius and the symbols used.

currents depend on time t as $e^{i\omega t}$ ($\omega = 2\pi f$ is the circular frequency, and f is the frequency, measured in Hz). At this the vibrator stays electrically thin, and the following inequalities are performed:

$$kr(s) \ll 1, \quad r(s) \ll 2L. \quad (1)$$

Then the tangential component of the scattered field on the vibrator surface in the cylindrical coordinate system $\{\rho, \varphi, s\}$ has the form:

$$E_\tau^{sc}(\rho, s) = E_s(\rho, s) \cos \psi + E_\rho(\rho, s) \sin \psi. \quad (2)$$

Here

$$\begin{aligned} E_s(\rho, s) &= \frac{\partial}{\partial s} \left[\frac{1}{\rho} \frac{\partial(\rho \Pi_\rho)}{\partial \rho} + \frac{\partial \Pi_s}{\partial s} \right] + k^2 \Pi_s, \\ E_\rho(\rho, s) &= \frac{\partial}{\partial \rho} \left[\frac{1}{\rho} \frac{\partial(\rho \Pi_\rho)}{\partial \rho} + \frac{\partial \Pi_s}{\partial s} \right] + k^2 \Pi_\rho, \end{aligned}$$

Π_s and Π_ρ are the components of the Hertz's electrical vector, corresponding to the vibrator electrical current $\vec{J}(s) = \vec{e}_s J_s(s) + \vec{e}_\rho J_\rho(s)$, where \vec{e}_s , \vec{e}_ρ are unit vectors of the cylindrical coordinate system.

Assuming according to Eq. (1) $|J_\rho| \ll |J_s|$, $J_s \approx J$, transiting to the total derivative along the longitudinal coordinate s , and also taking into account that $\frac{dr(s)}{ds} = \tan \psi$, we, finally, obtain the integral-differential equation relatively to the $J(s)$ current for the impedance boundary condition on the vibrator surface:

$$\begin{aligned} & \left(\frac{d^2}{ds^2} + k^2 \right) \int_{-L}^L J(s') \frac{e^{-ik\tilde{R}(s,s')}}{\tilde{R}(s,s')} ds' \\ &= -\frac{i\omega}{\cos \psi} E_{0\tau}(s) - \tan \psi \frac{d}{ds} \left\{ r(s) \int_{-L}^L J(s') \frac{e^{-ik\tilde{R}(s,s')}}{\tilde{R}^3(s,s')} ds' \right\} + \frac{i\omega}{\cos \psi} z_i J(s), \end{aligned} \quad (3)$$

where $E_{0\tau}(s)$ is the tangential component of the electrical field of the impressed sources; $\tilde{R}(s, s') = \sqrt{(s - s')^2 + r^2(s)}$; z_i is the internal linear impedance of the vibrator. So, for example, for metal cylinders (σ is the metal conductivity, and Δ^o is the skin layer thickness) under the condition $r \gg \Delta^o$, z_i is determined by the relation $z_i = \frac{1+i}{2\pi r \sigma \Delta^o}$ (see Table 1).

Note that at $r(s) = \text{const} = r_0$, Equation (3) transforms into an equation for the current in an impedance vibrator of constant radius [12] with a quasi-one-dimensional core $\tilde{R}(s, s') = R(s, s') =$

$\sqrt{(s-s')^2 + r_0^2}$. One can show by direct differentiation with consecutive application of the condition (1) that the ratio takes place as in the $r(s) = r_0$ case:

$$\frac{d^2}{ds^2} \frac{e^{-ik\tilde{R}(s,s')}}{\tilde{R}(s,s')} \cong \frac{d^2}{ds'^2} \frac{e^{-ik\tilde{R}(s,s')}}{\tilde{R}(s,s')}, \quad (4)$$

and the second addendum in the right part of Equation (3) equals zero at coincidence of the integration and observation points ($s' = s$), i.e., it does not have peculiarity:

$$\text{tg}\psi \frac{d}{ds} \left\{ r(s) \int_{-L}^L J(s') \frac{e^{-ik\tilde{R}(s,s')}}{\tilde{R}^3(s,s')} ds' \right\} \cong \text{tg}\psi r(s) \int_{-L}^L J(s') (s-s')^3 \frac{e^{-ik\tilde{R}(s,s')}}{\tilde{R}^5(s,s')} ds' \Big|_{s=s'} = 0.$$

Let us extract the main part of the kernel of Equation (3), making the following identical transformations:

$$\int_{-L}^L J(s') \frac{e^{-ik\tilde{R}(s,s')}}{\tilde{R}(s,s')} ds' = J(s)\Omega(s) + \int_{-L}^L \frac{[J(s')e^{-ik\tilde{R}(s,s')} - J(s)]}{\tilde{R}(s,s')} ds'. \quad (5)$$

Here

$$\Omega(s) = \int_{-L}^L \frac{ds'}{\tilde{R}(s,s')} = \Omega + \tilde{\gamma}(s, r(s)),$$

$$\tilde{\gamma}(s, r(s)) = \ln \left\{ \left(\frac{r_0}{r_L} \right)^2 \frac{[(L+s) + \sqrt{(L+s)^2 + r^2(s)}] [(L-s) + \sqrt{(L-s)^2 + r^2(s)}]}{4L^2} \right\},$$

$\Omega = 2 \ln \frac{2L}{r_L} \gg 1$, r_0 and r_L are the radii of the vibrator in its centre and on its end, correspondingly. We note that the obtained problem natural large parameter Ω coincides with the wave resistance of the biconical antenna of infinite length, considered in the frames of the model of the homogeneous line, along which the TEM-wave propagates without reflections, at the $\psi \leq 10^\circ$ small angles with accuracy to the constant multiplier [1].

Using the equality in Eq. (4) and neglecting the current on the vibrator ends ($J(\pm L) = 0$) [3], we obtain the integral-differential equation, whose right part is proportional to the α small parameter:

$$\frac{d^2 J(s)}{ds^2} + k^2 J(s) = \alpha \left\{ \frac{i\omega}{\cos \psi} E_{0r}(s) + F[s, J(s)] - \frac{i\omega}{\cos \psi} \frac{Z_S}{2\pi r(s)} J(s) \right\}. \quad (6)$$

Here $\alpha = \frac{1}{2 \ln[r_L/(2L)]}$, ($|\alpha| \ll 1$), $Z_S = z_i 2\pi r(s)$ is the surface vibrator impedance,

$$\begin{aligned} F[s, J(s)] = & - \frac{dJ(s')}{ds'} \frac{e^{-ik\tilde{R}(s,s')}}{\tilde{R}(s,s')} \Big|_{-L}^L + [J''(s) + k^2 J(s)] \tilde{\gamma}(s, r(s)) \\ & + \int_{-L}^L \frac{\{ [J''(s') + k^2 J(s')] e^{-ik\tilde{R}(s,s')} - [J''(s) + k^2 J(s)] \}}{\tilde{R}(s,s')} ds' \\ & + \text{tg}\psi r(s) \left[\int_{-L}^L \frac{e^{-ik\tilde{R}(s,s')}}{\tilde{R}^3(s,s')} ds' \right] \left\{ \frac{dJ(s')}{ds'} \Big|_{-L}^L - \int_{-L}^L [J''(s) + k^2 J(s)] ds \right\}. \end{aligned} \quad (7)$$

The $J''(s)$ and $J''(s')$ expressions designate the second derivative due to the s and s' coordinates in the operator $F[s, J(s)]$, defining the vibrator own field.

2.2. Solution of the Current Integral Equation by the Averaging Method

Let us use the asymptotic averaging method, whose efficiency is described in [12] applicable to the boundary problems of such a kind, to obtain the approximate solution of Equation (6). We change the variables in order to reduce Equation (6) to the equations system of a standard kind with the small parameter [13, 14]:

$$\begin{aligned} J(s) &= A(s) \cos ks + B(s) \sin ks, \\ \frac{dJ(s)}{ds} &= -A(s)k \sin ks + B(s)k \cos ks, \quad \left(\frac{dA(s)}{ds} \cos ks + \frac{dB(s)}{ds} \sin ks = 0 \right), \\ \frac{d^2 J(s)}{ds^2} + k^2 J(s) &= -\frac{dA(s)}{ds} \sin ks + \frac{dB(s)}{ds} \cos ks, \end{aligned} \quad (8)$$

where $A(s)$ and $B(s)$ are the new unknown functions.

Then Equation (6) transits into the system of the integral-differential equations, unsolved relatively to the derivative:

$$\begin{aligned} \frac{dA(s)}{ds} &= -\frac{\alpha}{k} \left\{ \frac{i\omega}{\cos \psi} E_{0\tau}(s) + F \left[s, A(s), \frac{dA(s)}{ds}, B(s), \frac{dB(s)}{ds} \right] \right. \\ &\quad \left. - \frac{i\omega Z_s}{2\pi \cos \psi r(s)} [A(s) \cos ks + B(s) \sin ks] \right\} \sin ks, \\ \frac{dB(s)}{ds} &= +\frac{\alpha}{k} \left\{ \frac{i\omega}{\cos \psi} E_{0\tau}(s) + F \left[s, A(s), \frac{dA(s)}{ds}, B(s), \frac{dB(s)}{ds} \right] \right. \\ &\quad \left. - \frac{i\omega Z_s}{2\pi \cos \psi r(s)} [A(s) \cos ks + B(s) \sin ks] \right\} \cos ks. \end{aligned} \quad (9)$$

Making partial averaging along the s variable with the consistent use of the condition (1) in the equations system (9) further, we obtain the equations of the first approximation relative to the $\bar{A}(s)$ and $\bar{B}(s)$ averaged functions:

$$\begin{aligned} \frac{d\bar{A}(s)}{ds} &= -\alpha \left\{ \frac{i\omega}{k \cos \psi} E_{0\tau}(s) + \bar{F} [s, \bar{A}(s), \bar{B}(s)] \right\} \sin ks + \chi_v \bar{B}(s), \\ \frac{d\bar{B}(s)}{ds} &= +\alpha \left\{ \frac{i\omega}{k \cos \psi} E_{0\tau}(s) + \bar{F} [s, \bar{A}(s), \bar{B}(s)] \right\} \cos ks - \chi_v \bar{A}(s). \end{aligned} \quad (10)$$

Here $\chi_v = \frac{i\alpha}{r_L \cos \psi} \left(\frac{3}{2} - \frac{r_0}{2r_L} \right) \bar{Z}_S$ and at $r_L = r_0$, χ_v transits into $\chi = i \frac{\alpha \bar{Z}_S}{r_0}$ (the parameter, taking into account the vibrator surface impedance of the constant radius r_0),

$$\bar{F}[s, \bar{A}(s), \bar{B}(s)] = [\bar{A}(s') \sin ks' - \bar{B}(s') \cos ks'] \frac{e^{-ik\bar{R}(s,s')}}{\bar{R}(s,s')} \Big|_{-L}^L \quad (11)$$

is the vibrator own field, averaged along its length.

Integrating the equations system (10) with taking into consideration Eq. (11), we obtain the most general asymptotic expression for the current in the impedance vibrator of the variable radius:

$$\begin{aligned} J(s) &= \bar{A}(-L) \cos(\tilde{k}s + \chi_v L) + \bar{B}(-L) \sin(\tilde{k}s + \chi_v L) \\ &\quad + \alpha \int_{-L}^s \left\{ \frac{i\omega}{k \cos \psi} E_{0\tau}(s') + \bar{F}[s', \bar{A}, \bar{B}] \right\} \sin \tilde{k}(s - s') ds', \end{aligned} \quad (12)$$

where $\tilde{k} = k + \chi_v$. It is necessary to use the boundary conditions for the $J(\pm L) = 0$ current and the conditions of symmetry, coupled both with the method of the vibrator excitation and its configuration, to define four constants $\bar{A}(\pm L)$ and $\bar{B}(\pm L)$ in Eq. (12).

Let us limit ourselves by consideration of the symmetrical case: $E_{0\tau}(s) = E_{0\tau}(-s)$, $r(s) = r(-s)$. The expression for the current has the form with substitution of the obtained values of the constants in Eq. (12):

$$J(s) = \alpha \frac{i\omega}{k \cos \psi} \left\{ \int_{-L}^s E_{0\tau}(s') \sin \tilde{k}(s-s') ds' - \frac{\sin \tilde{k}(L+s) + \alpha P^s[kr(s), \tilde{k}(L+s)]}{\sin 2\tilde{k}L + \alpha P^s[kr\{s\}, 2\tilde{k}L]} \int_{-L}^L E_{0\tau}(s') \sin \tilde{k}(L-s') ds' \right\}, \quad (13)$$

$$P^s[kr(s), \tilde{k}(L+s)] = \int_{-L}^s \left\{ \frac{e^{-ik\tilde{R}[s', -L; r(s')]} \tilde{R}[s', -L; r(s')]}{e^{-ik\tilde{R}[s', L; r(s')]} \tilde{R}[s', L; r(s')]} \right\} \sin \tilde{k}(s-s') ds' \Big|_{s=L} = P^s[kr\{s\}, 2\tilde{k}L].$$

Let the vibrator be excited by normal incident plain electromagnetic wave with the amplitude E_0 : $E_{0\tau}(s) = E_0 \cos \psi$, and its radius is changed according to the following law: $r(s) = r_0 + |s| \tan \psi$. Then, finally:

$$J(s) = -\alpha \frac{i\omega}{k\tilde{k}} E_0 \frac{(\cos \tilde{k}s - \cos \tilde{k}L) + \alpha \left\{ \frac{\sin \tilde{k}L P^s[kr(s), \tilde{k}(L+s)]}{-[1 - \cos \tilde{k}(L+s)] P^s[kr\{s\}, \tilde{k}L]} \right\}}{\cos \tilde{k}L + \alpha P^s[kr\{s\}, \tilde{k}L]}, \quad (14)$$

$$P^s[kr\{s\}, \tilde{k}L] = \int_{-L}^L \frac{e^{-ik\sqrt{(L-s)^2 + r^2(s)}}}{\sqrt{(L-s)^2 + r^2(s)}} \cos \tilde{k}s ds.$$

It is suitable to characterize the scattering properties of passive vibrators in free space by the normalized back-scattering cross section (BSCS) σ/λ^2 [11], whose expression has the form in the considered case:

$$\frac{\sigma}{\lambda^2} = \frac{4\alpha^2}{\pi} \left| \frac{k}{\tilde{k}} \right|^4 \left| \frac{\sin \tilde{k}L}{\cos \tilde{k}L + \alpha P^s[kr\{s\}, \tilde{k}L]} - \tilde{k}L \right|^2. \quad (15)$$

Let us note that the current in the vibrator has both the symmetrical $J^s(s) = J^s(-s)$ and antisymmetrical $J^a(s) = -J^a(-s)$ components and $J(s) = J^s(s) + J^a(s)$ in a general case, at the incidence of the plain wave under the angle to the vibrator axis or when $r(s) \neq r(-s)$.

2.3. Numerical and Experimental Results

Figure 2 represents the plots of the BSCS dependencies of perfectly conducting ($\bar{Z}_S = 0$) biconical vibrator from its electrical length $2L/\lambda$ ($2L = \text{const} = 15 \text{ cm}$, $r_0 = 0.1 \text{ cm}$) for different angles ψ . It is seen that the passive scattering vibrator becomes more broadband (due to the level of $0.5(\sigma/\lambda^2)$, referred to the maximal value of BSCS) at the ψ angle increase. At this the $(2L/\lambda)_{res}$ resonant values change insufficiently, and the σ/λ^2 maximal values increase sufficiently in the second pick of the resonant curve. The analogous picture is observed in the case, when $\lambda = \text{const}$, as shown in Fig. 3: $\lambda = 10 \text{ cm}$, $r_0 = 0.0127 \text{ cm}$. Here the dotted curve and circles are the results obtained by the Hallen-King's iterations method, and the experimental data for the silvered conductor from [15] (the normalization of all curves is made to the maximal experimental value of BSCS in the first resonance), correspondingly. Thus one can make a conclusion (as noted in [1–3]) that both the passive scattering and receiving biconical vibrators can operate effectively in wider range of the waves electrical lengths than the vibrators of the constant radius at the practically unchanged $(2L/\lambda)_{res}$ value.

For example, for impedance vibrators, when taking into account the finite conductivity of the metal they are made of, their electrodynamic characteristics will change, correspondingly, in comparison with

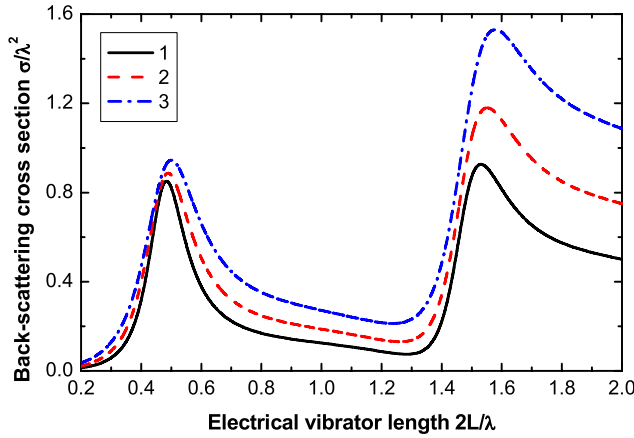


Figure 2. The σ/λ^2 dependences from the vibrator electrical length at $2L = 15$ cm, $r_0 = 0.1$ cm for different angles ψ : 1 — $\psi = 0^\circ$ ($r_L = 0.1$ cm); 2 — $\psi = 1.1^\circ$ ($r_L = 0.25$ cm); 3 — $\psi = 3.1^\circ$ ($r_L = 0.5$ cm).

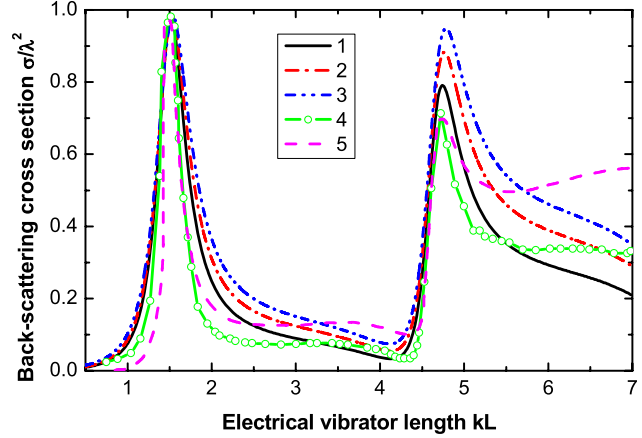


Figure 3. The σ/λ^2 dependences from kL at $\lambda = 10$ cm, $r_0 = 0.0127$ cm for different ratios r_L/r_0 : 1 — $r_L = r_0$; 2 — $r_L = 5r_0$; 3 — $r_L = 10r_0$; 4 and 5 — the experimental data and the calculated values at $r_L = r_0$ [15].

the case of perfect conductivity. Table 1 represents the calculated (due to Equation (15) and made by the variation method [15]) and also experimental data [15] of the maximal value of BSCS in the first resonance for copper and platinum thin wires with different radiuses of cross section. Obviously, the radius change along the vibrators length will lead to the same qualitative changes of the BSCS curves, which are given in Figs. 2, 3 for perfectly conducting biconical vibrators in these cases.

Table 1. The calculated values and the experimental data of the σ/λ^2 maximal value for thin metallic conductors.

r , cm	kr	Material	z_i [Ohm/cm]	σ/λ^2		
				Experiment [15]	Calculation [15]	Calculation, formula (15)
0.003×1.27	0.0024	Copper	$0.625 + i0.597$	0.768	0.805	0.804
0.002×1.27	0.0016	Platinum	$2.27 + i2.21$	0.690	0.725	0.744
0.003×1.27	0.0024	Platinum	$1.15 + i1.47$	0.727	0.760	0.774
0.005×1.27	0.0040	Platinum	$0.93 + i0.886$	0.763	0.788	0.792

It should be mentioned that the problem in question and its solution can be generalized for the case of the vibrator location in infinite material medium without principal difficulties.

3. IMPEDANCE BICONICAL VIBRATORS IN A RECTANGULAR WAVEGUIDE

3.1. Problem Formulation and the Initial Integral Equation

The structure in question and the symbols, accepted in the problem, are represented in Fig. 4(a). The thin vibrator of the variable radius $r(s)$ and length $2L$, which does not have the points of touching the waveguide walls (the symmetrical vibrator), is located in the rectangular waveguide of the section $\{a \times b\}$. The $\{0s\}$ local coordinate system is coupled with the vibrator, and the performance of the impedance boundary condition $E_\tau(s) = z_i(s)J(s)$ is required on its surface, where $E_\tau(s)$ is the full electrical field tangential component on the vibrator surface.

Let us limit ourselves, as it was earlier, by the linear law of the vibrator radius change along its length: $r(s) = r_0 + |s|\text{tg}\psi$, where $\text{tg}\psi = (r_L - r_0)/L$. The following integral-differential equation relative

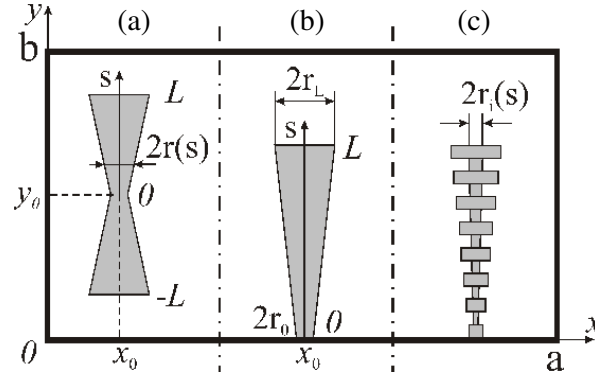


Figure 4. The problem formulation and the symbols used.

to the $J(s)$ electrical current in the vibrator (see Eq. (3)) is original for analysis in this case:

$$\begin{aligned} \left(\frac{d^2}{ds^2} + k^2 \right) \int_{-L}^L J(s') G_s[s, s'; r(s')] ds' &= -\frac{i\omega}{\cos \psi} E_{0\tau}(s) \\ + \text{tg} \psi \frac{d}{ds} \frac{\partial}{\partial r} \int_{-L}^L J(s') G_s[s, s'; r(s')] ds' &+ \frac{i\omega}{\cos \psi} z_i(s) J(s). \end{aligned} \quad (16)$$

Here $E_{0\tau}(s)$ is the impressed sources electrical field tangential component; s' is the local coordinate on the vibrator surface; $G_s[s, s'; r(s')]$ is the s -component of the Green's electrical function of the rectangular waveguide.

3.2. Solution of the Equation by the Generalized Method of Induced EMF

Let us apply the generalized method of induced EMF, approximating the current distribution due to the first term (which does not depend on the Green's function of the electrodynamic volume) of Equation (14), in the case of the vibrator symmetrical excitation $E_{0\tau}(s) = E_{0\tau}(-s)$ and under the condition that $z_i(s) = z_i(-s)$:

$$J(s) = J_0 f(s) = J_0 (\cos \tilde{k}s - \cos \tilde{k}L), \quad f(\pm L) = 0, \quad (17)$$

where $\tilde{k} = k - \frac{i2\pi z_i^{av}}{Z_0 \Omega} \left[\frac{1}{\cos \psi} \left(\frac{3}{2} - \frac{r_0}{2r_L} \right) \right]$, $\Omega = 2 \ln \frac{2L}{r_L}$, $z_i^{av} = \frac{1}{2L} \int_{-L}^L z_i(s) ds$ is the mean value of the internal impedance along the vibrator length, and J_0 is the current unknown amplitude. As a result, the searched expression for the current at the vibrator excitation by the TE_{10} -wave (with amplitude E_0) has the form:

$$J(s) = -\frac{i\omega}{k\tilde{k}} E_0 \sin \frac{\pi x_0}{a} \frac{(\sin \tilde{k}L - \tilde{k}L \cos \tilde{k}L)(\cos \tilde{k}s - \cos \tilde{k}L)}{Z_\psi^W(\tilde{k}L) + \text{tg} \psi \tilde{Z}_\psi^W(\tilde{k}L) + F_{z\psi}^W(\tilde{k}L)}. \quad (18)$$

The symbols are accepted in Equation (18):

$$Z_\psi^W(\tilde{k}L) = \frac{1}{2k} \int_{-L}^L f(s) \left(\frac{d^2}{ds^2} + k^2 \right) \left[\int_{-L}^L f(s') G_s[(s, s'; r(s'))] ds' \right] ds, \quad (19)$$

$$\tilde{Z}_\psi^W(\tilde{k}L) = \frac{1}{2k} \int_{-L}^L f(s) \frac{d}{ds} \frac{\partial}{\partial r} \left[\int_{-L}^L f(s') G_s[(s, s'; r(s'))] ds' \right] ds, \quad (20)$$

$$F_{z\psi}^W(\tilde{k}L) = -\frac{i}{r(s)} \int_{-L}^L f^2(s) \bar{Z}_S(s) ds, \quad (21)$$

$\bar{Z}_S(s) = \bar{R}_S(s) + i\bar{X}_S(s) = 2\pi r(s)z_i(s)/Z_0$, ($Z_0 = 120\pi$ [Ohm]) is the normalized complex surface impedance of the vibrator, distributed along it due to the definite law $\bar{Z}_S(s) = \bar{Z}_S\phi(s)$, where $\phi(s)$ is the set function. The electric Green's function for the structure under consideration will have the form (s -component):

$$G_s[s, s'; r(s')] = \frac{4\pi}{ab} \sum_{m=1}^{\infty} \sum_{n=0}^{\infty} \frac{\varepsilon_n}{k_z} e^{-k_z r(s')} \sin^2 k_x x_0 \cos k_y (y_0 + s) \cos(y_0 + s' \cos \psi), \quad (22)$$

where $\varepsilon_n = \begin{cases} 1, & n = 0 \\ 2, & n \neq 0 \end{cases}$, $k_x = \frac{m\pi}{a}$, $k_y = \frac{n\pi}{b}$, $k_z = \sqrt{k_x^2 + k_y^2 - k^2}$, m and n are the integers.

Then, finally, we obtain after the substitution of Eq. (22) into Eqs. (19) and (20):

$$Z_{\psi}^W(\tilde{k}L) = \frac{8\pi}{ab} \sum_{m=1}^{\infty} \sum_{n=0}^{\infty} \frac{\varepsilon_n(k^2 - k_y^2)\tilde{k}}{kk_z(\tilde{k}^2 - k_y^2)} e^{-k_z r_0} \sin^2 k_x x_0 \cos^2 k_y y_0 \\ \times [\sin \tilde{k}L \cos k_y L - (\tilde{k}/k_y) \cos \tilde{k}L \sin k_y L] F_{\psi}(\tilde{k}L), \quad (23)$$

$$\tilde{Z}_{\psi}^W(\tilde{k}L) = \frac{4\pi}{ab} \sum_{m=1}^{\infty} \sum_{n=1}^{\infty} \frac{\tilde{k}^2}{k(\tilde{k}^2 - k_y^2)} e^{-k_z r_0} \sin^2 k_x x_0 \\ \times [\cos \tilde{k}L (\cos k_y L - 1) + (k_y/\tilde{k}) \sin \tilde{k}L \sin k_y L + (k_y/\tilde{k})^2 (\cos k_y L - 1)] F_{\psi}(\tilde{k}L), \quad (24)$$

where

$$F_{\psi}(\tilde{k}L) = \frac{1/2}{(\tilde{k} + k_y)^2 + (k_z \operatorname{tg} \psi)^2} \left\{ e^{-k_z L \operatorname{tg} \psi} [(\tilde{k} + k_y) \sin(\tilde{k} + k_y)L - k_z \operatorname{tg} \psi \cos(\tilde{k} + k_y)L] + k_z \operatorname{tg} \psi \right\} \\ + \frac{1/2}{(\tilde{k} - k_y)^2 + (k_z \operatorname{tg} \psi)^2} \left\{ e^{-k_z L \operatorname{tg} \psi} [(\tilde{k} - k_y) \sin(\tilde{k} - k_y)L - k_z \operatorname{tg} \psi \cos(\tilde{k} - k_y)L] + k_z \operatorname{tg} \psi \right\} \\ - \frac{\cos \tilde{k}L}{k_y^2 + (k_z \operatorname{tg} \psi)^2} \left\{ e^{-k_z L \operatorname{tg} \psi} [k_y \sin k_y L - k_z \operatorname{tg} \psi \cos k_y L] + k_z \operatorname{tg} \psi \right\}.$$

For the impedance vibrator, drawn in Fig. 4(c), at $[r(s)/r_i(s)] = \text{const}$ we have:

$$F_{z\psi}^W(\tilde{k}L) = -\frac{i\bar{Z}_S}{2 \cos \psi \tilde{k}r_0} \left[\tilde{k}L(2 + \cos 2\tilde{k}L) - \frac{3}{2} \sin 2\tilde{k}L \right], \quad (25)$$

where \bar{Z}_S is defined by the formula $\bar{Z}_S = i\bar{X}_S = ikr \ln(r/r_i)$ without taking into consideration the finite conductance of the metal.

Let us note that, as before, the expression for the current also has the form of Eq. (18) for the asymmetrical vibrators, drawn in Figs. 4(b), (c), and it is necessary to make substitutions $y_0 = 0$, $b \rightarrow 2b$ in Equations (23), (24). We shall consider the asymmetrical vibrator, for which the S_{11} reflection coefficient along the field in the waveguide equals, further:

$$S_{11} = -\frac{4\pi i}{abk\gamma} \left(\frac{k}{\tilde{k}} \sin \frac{\pi x_0}{a} \right)^2 \frac{(\sin \tilde{k}L - \tilde{k}L \cos \tilde{k}L)^2 e^{2i\gamma z}}{Z_{\psi}^W(\tilde{k}L) + \operatorname{tg} \psi \tilde{Z}_{\psi}^W(\tilde{k}L) + F_{z\psi}^W(\tilde{k}L)}, \quad (26)$$

where $\gamma = \sqrt{k^2 - (\pi/a)^2}$ is the propagation constant of the TE_{10} -wave.

Note that the summation in Eqs. (23), (24) was performed with an accuracy of 1% (compared to the first discarded term of the series). Due to the presence of a multiplier $e^{-k_z r_0}$, the number of considered members of the series is several tens.

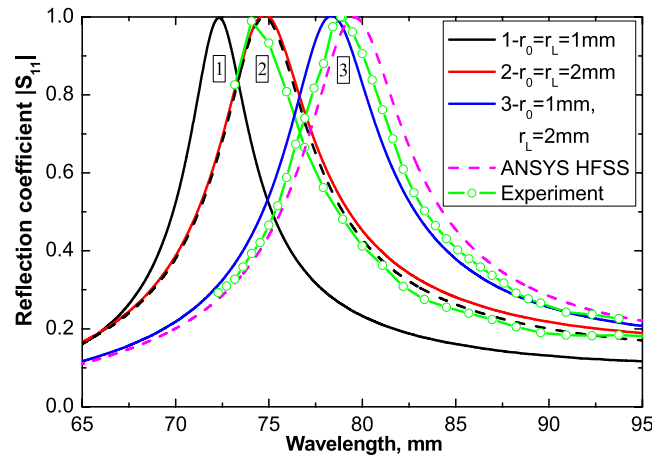


Figure 5. The module calculation and experimental dependences of the reflection coefficient from the wavelength for the perfectly conducting vibrators at the constant and variable radiuses of their cross section: 1, 2, 3 — calculation due to the formula (26), 4 — calculation due to the program “ANSYS HFSS”, 5 — experimental data.

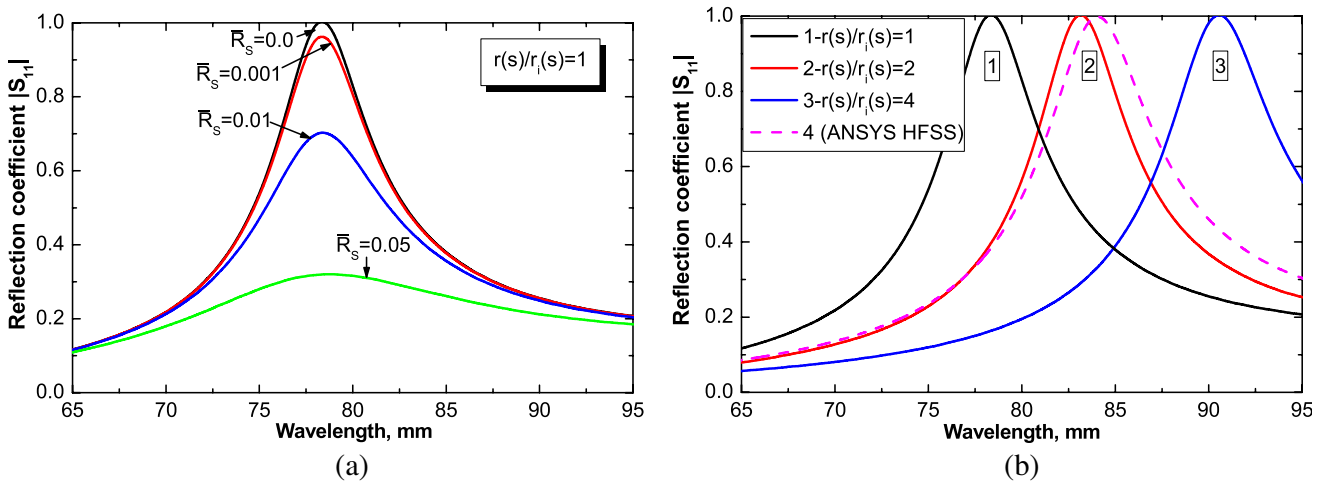


Figure 6. The module dependences of the reflection coefficient from the wavelength for the perfectly conducting and impedance vibrators at the variable radius ($r_0 = 1.0$ mm, $r_L = 2.0$ mm) of their cross section: 1, 2, 3 — calculation due to the formula (26), 4 — calculation due to the program “ANSYS HFSS”.

3.3. Numerical and Experimental Results

Figures 5, 6 represent the dependences of the $|S_{11}|$ value from the wavelength for the perfectly conducting (Fig. 5) and impedance (Fig. 6) asymmetrical vibrators at the following general parameters $\{a \times b\} = 58 \times 25 \text{ mm}^2$, $L = 15.0$ mm, $x_0 = a/8$.

As it is seen from the plots, the value of the λ_{res} resonant wavelength increases (the curves 3 in Fig. 5) in comparison with the conductors of the constant radius (the curves 1, 2 in Fig. 5) for the conical vibrator, and moreover, the radii of the latter is equal to a smaller (the curve 1) and a larger (the curves 2) radii of the conical vibrator, correspondingly. To our minds, this interesting fact is explained by that the definite redistribution of energy of the near reactive fields between the E - and H -kinds of waveguide modes, connected with the occurrence of some angle ψ between the axis $\{Oy\}$ of the waveguide and $\{Os'\}$ on the surface of the conductor, as this takes place at the slope of the regular vibrator axis in the



Figure 7. The experimental layouts.

cross section plane of the rectangular waveguide, occurs for the conical vibrator. As it follows from the plots in Fig. 6, the availability of impedance of the real kind \bar{R}_S in the conical vibrator decreases the values of $|S_{11}|$ (Fig. 6(a)), and that of the impedance of the inductive kind (Fig. 4(c) — the corrugated conductor) increases λ_{res} much larger (the curves 2, 3 in Fig. 6(b)). Let us note the comparison of calculation results with the experimental data (photo of the experimental layouts is shown in Fig. 7), and the calculation with the use of the program “ANSYS HFSS” (the circles and dotted lines in Figs. 5, 6) has been done in order to check the rightness of the proposed approach to the set problem solution.

4. CONCLUSION

The calculated and experimental results presented in the article on the study of electrodynamic structures with impedance biconical vibrators can be useful in the development of antenna-waveguide devices (including coaxial-waveguide transitions) with new electrodynamic characteristics. The comparison of calculated and experimental data confirms the adequacy of the proposed mathematical models to real physical processes. We note that the proposed approach to solving problems can be extended to spherical surfaces with impedance biconical monopoles [16], as well as to combined slot-vibrator structures [17], without any particular fundamental difficulties.

REFERENCES

1. Schelkunoff, S. A., “Theory of antennas of arbitrary size and shape,” *Proc. IRE*, Vol. 29, 493–521, 1941.
2. Tai, C. T., “On the theory of biconical antennas,” *Journal Applied Phys.*, Vol. 19, 1155–1160, 1948.
3. Schelkunoff, S. A., *Antennas Theory and Practice*, Facsimile Publisher, 1952.
4. Wu, T. T. and R. W. P. King, “The tapered antenna and its application to the junction problem for thin wires,” *IEEE Trans. Antennas Propag.*, Vol. 24, 42–45, 1976.
5. Saoudy, S. A. and M. Hamid, “Input admittance of a biconical antenna with wide feed gap,” *IEEE Trans. Antennas Propag.*, Vol. 38, 1784–1790, 1990.
6. Sandler, S. S. and R. W. P. King, “Compact conical antennas for wide-band coverage,” *IEEE Trans. Antennas Propag.*, Vol. 42, 436–439, 1994.
7. Wong, K.-L. and S.-L. Chien, “Wide-band cylindrical monopole antenna for mobile phone,” *IEEE Trans. Antennas Propag.*, Vol. 53, No. 8, 2756–2758, 2005.
8. Song, C., Y. Huang, J. Zhou, P. Carter, S. Yuan, Q. Xu, and Z. Fei, “Matching network elimination in broadband rectennas for high-efficiency wireless power transfer and energy harvesting,” *IEEE Trans. Industrial Electronics*, Vol. 64, 3950–3961, 2017.

9. Dumin, O., P. Fomin, V. Plakhtii, and M. Nesterenko, "Ultrawideband combined monopole-slot radiator of Clavin type," *Proc. XXVth International Seminar on Direct and Inverse Problems of Electromagnetic and Acoustic Wave Theory*, 32–36, Tbilisi, Georgia, 2020.
10. Fomin, P., O. Dumin, V. Plakhtii, and M. Nesterenko, "UWB antenna arrays with the monopole-slot radiator of Clavin type," *Proc. IIIth Ukraine Conf. on Electrical and Computer Engineering*, 258–261, Lviv, Ukraine, 2021.
11. Scolnik, M. I., *Radar Handbook*, McGraw-Hill Book Company, 1970.
12. Nesterenko, M., "Analytical methods in the theory of thin Impedance vibrators," *Progress In Electromagnetics Research B*, Vol. 21, 299–328, 2010.
13. Bogoliubov, N. N. and Y. A. Mitropolsky, *Asymptotic Methods in the Theory of Nonlinear Oscillations*, Gordon and Breach, NY, 1961.
14. Philatov, A. N., *Asymptotic Methods in the Theory of Differential and Integral-differential Equations*, PHAN, Tashkent, 1974 (in Russian).
15. Dike, S. H. and D. D. King, "The absorption gain and back-scattering cross section of the cylindrical antenna," *Proc. IRE*, Vol. 40, 853–860, 1952.
16. Penkin, Yu. M., V. A. Katrich, M. V. Nesterenko, S. L. Berdnik, and V. M. Dakhov, *Electromagnetic Fields Excited in Volumes with Spherical Boundaries*, Springer Nature Switzerland AG, Cham, Switzerland, 2019.
17. Nesterenko, M. V., V. A. Katrich, Yu. M. Penkin, S. L. Berdnik, and O. M. Dumin, *Combined Vibrator-Slot Structures: Theory and Applications*, Springer Nature Switzerland AG, Cham, Switzerland, 2020.